IEEE Access
Multidisciplinary ⋮ Rapid Review ⋮ Open Access Journal

Received 14 December 2022, accepted 4 January 2023, date of publication 10 January 2023, date of current version 18 January 2023.

Digital Object Identifier 10.1109/ACCESS.2023.3235896

RESEARCH ARTICLE

Evolutionary Optimization of Antennas for Structural Health Monitoring

DOMINIK MAIR[1], (Member, IEEE), MORITZ FISCHER[1], JULIAN KONZILIA[2], MICHAEL RENZLER[1], AND THOMAS USSMUELLER[1], (Senior Member, IEEE)

[1]Department of Mechatronics, University of Innsbruck, 6020 Innsbruck, Austria
[2]Unit of Concrete Structures and Bridge Design, University of Innsbruck, 6020 Innsbruck, Austria

Corresponding author: Michael Renzler (michael.renzler@uibk.ac.at)

This work was supported in part by the Austrian Research Promotion Agency within the BridgeTEX Project under Grant 871549, in part by the European Regional Development Fund (ERDF) within the K-Regio Project "SafeAviationTyrol," and in part by the Austria Wirtschaftsservice Gesellschaft (AWS) within the prototype funding and the University of Innsbruck under Grant P2372773.

ABSTRACT Monitoring and surveillance of buildings, especially in critical infrastructure is crucial to increase the lifetime of such structures. This is due to the fact, that concrete buildings, like bridges or road tunnels are prone to corrosion due to their exposure to the elements. For this task, wireless sensor nodes can be employed in structural health monitoring. In the last few years passive RFID sensors have been proposed to gather data from inside concrete structures. However, designing antennas which are operational inside concrete to transmit data from the sensor node to the outside world is extremely challenging, due to the fact that the performance of antennas is extremely depended on their surrounding material. In this work, the fully automatized design of an antenna for the UHF band in concrete with varying electrical properties is demonstrated. Using a novel multi-objective optimization method, the antennas are operational over a wide range of dielectric properties of the surrounding materials. In contrast to conventional approaches, no air spacers or boxes are needed around the antenna. The antenna parameters have been carefully obtained during the curing and drying process, in an outdoor like environment with 65 % relative humidity. After 157 days of drying, a reflection coefficient of −13 dB and an antenna gain of −8.4 dBi is achieved, at a water content of the concrete of 4.2 % by mass.

INDEX TERMS Antennas, genetic algorithms, structural engineering, remote monitoring.

I. INTRODUCTION

Damages due to corrosion are a serious problem for infrastructure and are an immense cost factor in public spending, with estimated global costs of 2.5 trillion US dollars in 2013 [1]. The lack of corrosion control strategies can not only cause secondary costs by outages, but also severe accidents. This can lead to a threat of public safety, as seen in the collapse of the Ponte Morandi bridge in 2018, that took the life of 43 persons. Although, the exact details of the collapse are still in discussion [2], the main reason for this accident is expected to be corroded steel rebars [3]. In general, corrosion of steel rebars is the primary reason for failures in other reinforced concrete structures. Therefore, it is assumed that proper corrosion management could result in cost savings of up to 35 % [1].

Thus, an efficient corrosion monitoring and management is indispensable and highly demanded, to prevent such tragedies. Therefore, it is desirable to have as good as possible insight into the building by observing important parameters like moisture and chloride ion concentration [4].

In order to use non-destructive measuring techniques, the trend is moving towards wireless sensor technology [5], [6], [7], [8]. One major challenge with concrete buildings is that they have to be monitored over decades, which makes the use of embedded, battery based solutions unfeasible. Technologies such as passive high frequency (HF) radio frequency identification (RFID) can circumvent this disadvantage [9]. Although, HF RFID can be used to transmit data and power to and from sensor nodes embedded in

The associate editor coordinating the review of this manuscript and approving it for publication was Tutku Karacolak.

This work is licensed under a Creative Commons Attribution 4.0 License. For more information, see https://creativecommons.org/licenses/by/4.0/

concrete, their communication range is typically very limited, due to the underlying working principle based on electromagnetic induction. In contrast, ultra high frequency (UHF) RFID is operating at a higher frequency and is based on the transmission of electromagnetic waves using antennas. This allows for higher communication distances, however, propagating waves are highly attenuated traveling through conductive materials and reflections occur at the transition between two different materials. Jiang et. al. performed a theoretical investigation on the amount of loss accompanied with electromagnetic waves travelling from air into a concrete wall in the frequency range of 1 MHz up to 1 GHz [10]. It can be seen that for installation depths of a few centimeters, losses due to reflections at the boundary dominate. As these losses due to reflections are significantly increasing towards lower frequencies, UHF RFID, which operates between 860–960 MHz, is the method of choice.

For any wireless data or power transmission, a suitable antenna is necessary. To operate within a material, the antenna must be adapted to the properties of said material. However, relevant properties of concrete like conductivity σ and permittivity ϵ_r are highly dependent on the specific type of concrete and its moisture content. Therefore, these parameters also depend on the specific structure in which the concrete is used and on time dependent environmental conditions like air humidity, temperature and amount of water near the concrete, such as seasonal effects. Inevitably, this leads to the conclusion that an antenna designed for operation within concrete has to be operational under a variety of different circumstances. In literature values of $\varepsilon_r = 5$ to 8 and $\sigma = 0.01$ to 0.1 for a frequency of 1 GHz are mentioned for concrete with respect to moisture content [11], which agree well with data from other sources [12], [13], that use similar concrete mixtures and compressive strengths. Nevertheless, this wide range of dielectric properties makes it extremely challenging to design an antenna suitable for reliable operation inside concrete. Additionally, the aforementioned values were retrieved after an initial drying stage. Therefore, some authors stated that higher values can be expected within the curing phase of the concrete, due to incomplete hydration [11].

An approach that has been presented several times in literature, is to design an antenna for operation in air and to get rid of the concrete's unwanted influences by mechanical separation (e.g air cavities, styrofoam spacers or plastic boxes) [14], [15], [16], [17], [18], [19]. However, such measures inevitably lead to potential mechanical weaknesses, which can in turn lead to water penetration, and thus contribute to increased corrosion. Aside from these structural issues, most of the mentioned publications either do not present measurements of antenna parameters like the absolute gain or do not compare them to simulations.

Jeong et al. reported a microstrip antenna inside a plastic housing with an additional metal cavity, used as a reflector cup, that yields comparatively high gain values [17]. However, due to the housing, the antenna is not in direct contact with the concrete and the metal cavity provides shielding to the other spatial directions. Furthermore, the metal cavity is prone to favour water ingress and therefore, can lead to accelerated corrosion. A patch antenna is presented by Shams et al. [14], where a surrounding air box is employed to reduce effects of the concrete environments. However, the presented simulated data could not be confirmed by measurements. In addition to that, little to none information on concrete related parameters such as composition, moisture content, drying time and environmental conditions are given, which heavily affect the performance of an antenna. For the monitoring of critical infrastructure, it is therefore necessary to investigate the antenna parameters for concrete at typical outdoor conditions. Concrete dried for long time in indoor laboratories, may result in underestimation of effects due to moisture.

This paper presents a method for designing an antenna capable of proper functionality within all specified material parameters of concrete, thus eliminating the need for an additional encapsulation. Using the presented method, it is possible to design an antenna for UHF RFID sensors, which can be manufactured on a single substrate layer and directly embedded into concrete, capable of transmitting data for all expected electrical parameters of concrete. To develop such a structure, evolutionary optimized pixelated antennas with shifted cross shaped elements are employed [20]. In order to optimize for the multiple goals of different electrical parameters of concrete, the previously reported method is enhanced for multi-objective optimization (MOO) with the help of Pareto optimization. The optimized antenna was manufactured, and embedded at an installation depth of 2 cm in a concrete block with a size of 30 × 30 × 17.5 cm. All antenna parameters have been thoroughly characterized by measurements and compared to simulations with respect to moisture content over the course of 6 months. In order to control environmental conditions, the blocks have been dried in a climate chamber at constant temperature and humidity.

This is the first report on antennas that are completely submerged in another material, where the materials varying electrical parameters have been included in the simulation.

II. METHODS

A. EVOLUTIONARY PIXELATED ANTENNA DESIGN

In the presented work a fully automated antenna design and optimization strategy is employed. Therefore, so called pixelated antennas are used, that have been optimized using a genetic algorithm [21]. The specific implementation has been discussed in detail previously [20], therefore only a short summary is given here. Improvements of the technique towards an optimization for multiple goals, are described in more detail in section II-B.

For the optimization, a predefined 2-dimensional region is divided into pixels, whose binary attributes are either

conductive or non-conductive. Therefore, the antenna can be represented as a binary sequence containing all the pixels, i.e 1's (conductive) or 0's (non-conductive) elements. In a first step, the genetic algorithm generates an initial population of individual antennas, by randomly selecting values for each pixel. In order to evaluate each of the antennas, a simulation, using the software package Sonnet is performed. Sonnet is a 2.5 D simulator, using the method of moments (MoM), which allows for extremely fast simulation times for the presented scenario. The simulations yield antenna parameters, that are being used as target functions by the genetic optimizer in turn. In this study, the simulated reflection coefficient S_{11} is used to select best performing individuals as parents for the next generation. Therefore, new individuals are created by randomly selecting attributes from parent individuals (crossover) and an additional random ''mutation'' process.

The optimization is implemented in Matlab, which generates appropriate simulation files via a Sonnet plugin. The pixels are cross shaped to avoid singularities [20]. Therefore, the generated final antenna structure can easily be manufactured with a typical circuit board manufacturing process.

B. MULTI-OBJECTIVE OPTIMIZATION ENHANCEMENT

In order to optimize pixelated antennas for more than one objective function, the previously reported optimization procedure is expanded to introduce multiple goals. The approach used in this publication, is a variant of the controlled, elitist genetic algorithm NSGA-II, which is supported by the Matlab function *gamultiobj()* [22].

In contrast to only elitist genetic approaches, controlled algorithms do not only favor individuals with better fitness functions, but also those that increase the diversity of the population. First, the initial population is generated with a uniform distribution (i.e. 50% of the area is taken up by 1's). This population is simulated to calculate the fitness vector containing each goal's values like antenna gain, reflection coefficient or efficiency, for all individuals. This is followed by the selection of the parents, which are used as templates for the next generation. For the selection of parents, two measures are evaluated: an individual's rank and the crowding distance.

The rank is defined by the dominance of an individual. An individual A dominates an individual B, if the solution of A is not worse than B in all objective functions or if the solution of A is strictly better than B in at least one objective function. A lower rank has a higher chance of selection.

The crowding distance is a measure of the diversity of the population. An individual solution's crowding distance is calculated by enclosing it with a cuboid whose corners are the neighboring solutions within the same rank. This cuboid's half circumference is the crowding distance value.

Using these two measures, it is possible to run a binary tournament selection, where two individuals are selected to compete against each other. An individual wins and is selected as a parent, if its solution has a lower rank. If they share the same rank, the individual with the higher crowding distance wins.

After the parents are selected, children are created by mutation and crossover functions. The children and the initial population are gathered into an extended population. The ranks and crowding distances are again computed for the extended population in order to trim the population down to the same size as before. Again, the individuals of this population are selected by the rank and crowding distance and the resulting population is used to create (grand-)children. At this point, the algorithm is continued iteratively until the parameter spread - a measure for the movement of the Pareto set - is not changing anymore.

The output of this procedure is not one, but a variety of different solutions. These solutions are called the Pareto set. For this work the solution with the lowest average reflection coefficient is selected. Therefore, the root mean square (RMS) is calculated over all defined goals.

C. ANTENNA MEASUREMENTS

Measurements were done inside an anechoic chamber. Fig.1-a) shows the setup inside the chamber. The distance between the antenna inside the concrete and the reference antenna is 2 m. An additional styrofoam mount for the concrete blocks was built and placed onto a rotary disk inside the chamber, which allows 360° rotation around the vertical axis. By manually placing the block in various orientations on the table, different cuts of the gain pattern are measured, as shown in Fig.1-b1) and Fig.1-b2). In order to ensure, that the embedded antenna is centered horizontally (Fig.1-b2), the slit in the styrofoam mount is slightly off-center, to account for the placement of the antenna inside the concrete block. Fig.1-c1) shows the connection of a balun to the embedded antenna for gain measurements, whereas Fig.1-c2) shows the testfixture for the impedance measurements. A thin 3d printed shield is positioned around the connections of the antenna to prevent concrete from touching the feedpoints of the testfixture for impedance measurements and to prevent concrete from penetrating the balun structure which would render the balun useless.

1) IMPEDANCE MEASUREMENT

Due to the asymmetrical balanced nature of the produced antennas, the method published by Qing et al. is chosen for the measurement of the antenna parameters [23]. This allows a broadband measurement of the scattering parameter. A differential fed asymmetrical balanced antenna can be represented by a two port network. Therefore, it is possible to determine the antenna's differential impedance Z_D by measuring the two-port scattering parameters.

Prior to the measurement, the VNA is calibrated using TOSM calibration [Rohde und Schwarz, ZV-Z170]. A test fixture, consisting of two semi-rigid coaxial cables to connect both arms separately, is built beforehand and is set in concrete together with the antenna, with the connector leading

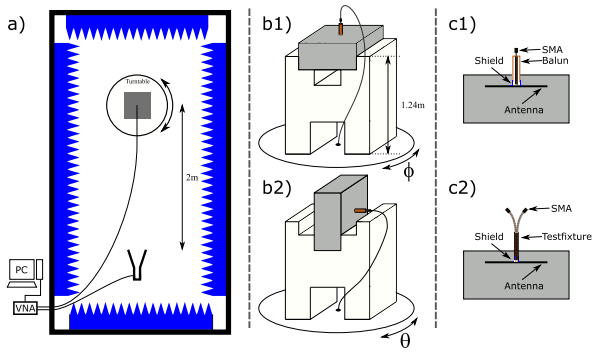

FIGURE 1. Schematic presentation of the measurement setup: a) placement of the concrete block inside the chamber in relation to the reference antenna, b) placement of the concrete block on the styrofoam mount for gain measurements, c) connections for gain (c1) and impedance measurement (c2).

FIGURE 2. Photograph of the actual setup. In the front the styrophoam mount with the concrete block can be seen, in the back of the aneochic chamber the reference antenna is shown.

outside. In order to eliminate the influence of the test fixture, a standard port extension technique of the employed VNA using shorted test fixture connectors is used. Hence, the data of the short measurement has to be taken before attaching the antenna and casting of the concrete blocks.

2) GAIN MEASUREMENT

In order to verify the capability of radiating electromagnetic fields, the antenna gain patterns are obtained at the antenna's operating frequency. In order to measure the antenna's total system gain patterns, we used a horn antenna as a reference inside an anechoic chamber.

This measurement is performed twice (horizontal and vertical reference antenna) to obtain the total system gain. Due to the asymmetrical, differential structure of the optimized antennas, a quarterwave sleeve Balun has to be employed [24]. Otherwise, unbalanced currents occur on the coaxial cable, making the coaxial cable no longer shielded but rather a radiating element, which leads to errors such as pattern squint. For final measurements, the quarter wave balun is soldered to the antenna and set into concrete together with it.

D. CONCRETE PREPARATION AND MOISTURE MEASUREMENT

In order to test the Antenna inside concrete, box shaped blocks with the dimensions 30 cm × 30 cm × 17.5 cm are cast. Thereby, the block dimension exceeds one wavelength in each direction, even for the lowest expected permittivity value of $\epsilon_r = 5$.[1]

The concrete used in civil infrastructure must be highly adapted to the environmental requirements of the specific application and the associated exposure conditions. To catalog the environmental conditions, EN 206 lists so-called exposure classes [25], which are defined for Austria in OENORM B 4710 [26]. Of particular importance for civil infrastructure are corrosive attack (XC for carbonatization and XD for chloride attack) and freeze-thaw attack (XF). In order to meet the required properties, ÖNORM B 4710 specifies the minimum quantity of cement and the water content expressed by the so-called w/cm ratio [26]. This ratio describes the relationship between the amount of water (w) and the amount of cementitious material (cm) per cubic meter of concrete.

TABLE 1. Concrete mixture.

Component	Type	Unit	Quantity
Cement	CEM II/A-M 42.5 N	$\mathrm{kg\,m^{-3}}$	414
Aggregate	GK 0/8	$\mathrm{kg\,m^{-3}}$	1658
Additive	Superplasticicer	$\mathrm{kg\,m^{-3}}$	3,2
Water Content	[-]	w/cm	0.45

In order to simulate realistic conditions, a specific type of concrete is selected, that can be used in civil infrastructure: it must have a high frost resistance and a high resistance to chloride penetration. The mixture used in the presented case is given in Tab.1. As a binder, Portland composite cement is used. In addition to Portland cement, it contains additives in the form of granulated blastfurnace slag and limestone powder. By replacing part of the Portland cement with additives, the ecological footprint of the cement and the heat of hydration can be reduced. As a result, the occurring restraint forces are decreased and early cracking of the concrete is reduced [27], [28]. This is particularly important for massive structural components with high-performance requirements in civil infrastructure. The used aggregate has a maximum grain size of 8 mm. In addition, the concrete contains air-entraining agents and superplasticizers to ensure the intended properties and workability. The obtained concrete has the properties C25/30 XC4/XD3/XF4 according to OENORM B 4710 [26].

In order to ensure a consistent quality of the concrete and to verify the conformity of the fresh concrete with the planned mixture, fresh concrete tests are carried out. With the help

[1]The wavelength λ in a material is shortened compared to the vaccum wavelenght λ_0: $\lambda = \lambda_0/\sqrt{\epsilon_r}$. At 868 MHz and $\epsilon_r = 5$, $\lambda = 34.54\,\mathrm{cm}/\sqrt{5}$.

of these tests, deviations from the desired properties can be detected at an early stage and undesirable effects can be prevented [25]. The testing regime to be applied, is defined by EN 12350 [29] and ONR 23303 [30] respectively, which is applicable in Austria. In this context, the fresh concrete parameters of bulk density, air content, water content and consistency are tested. The properties of the concrete are shown in Table 2. Only minor deviations from the design mixture are observed.

The test fixtures for antenna measurements are attached to the antennas and then partially also set into concrete, with connectors leading to the outside of the concrete block. Three different types of blocks have been cast: one containing a test fixture for impedance measurements (section II-C1), one containing the balun for gain measurements (section II-C2) and one block as a reference for measuring temperature and moisture content. In case the fragile test fixtures are damaged and additionally, to confirm measurement results, two blocks of each type are cast. The antennas are all fixed at a depth of 2 cm below the surface.

In order to observe the antenna's properties with respect to water content, regular measurements have been performed. Holes have been drilled into the reference blocks at different spots and depths. The drilling dust is weighted right after drilling and dried for at least 24 h at 105 °C. From the weight difference, the moisture content is calculated for different depths. In the course of this study, drills at depths of 1.5 cm to 3.5 cm and 3.5 cm to 7.5 cm have been evaluated separately. This allows to detect any significant differences in moisture at the antenna's depth compared to the block center, but the measured difference has been found to be negligible. Additionally, both reference blocks are drying equally within error margins. All data within this work is given as percent by mass, as this is the one typically used in concrete technologies. However, it should be noted that other studies on dielectric properties often use percent water by volume, when comparing different concrete recipes.

After casting, the blocks are wrapped in polyethylene for 24 hours and afterwards all 6 blocks are dried in a climate chamber at a fixed temperature of 22 °C and a humidity of 65 %. The maximum temperature measured inside the two reference blocks during initial drying is 39 °C, 9 h after casting. For measurement of the antenna parameters, all blocks are taken out of the climate chamber and are brought to the antenna measurement chamber. After 157 days of drying under controlled conditions, the blocks have been dried at 40 °C in the oven for 11 days. Thereby, a moisture content close to or slightly below the expected equilibrium moisture at the drying conditions is achieved.

III. RESULTING ANTENNA

As mentioned earlier, the dielectric properties of concrete heavily depend on the moisture content. Therefore, we selected a minimum of the reflection coefficient in the range of $\varepsilon_r = 5$ to 8 and $\sigma = 0.01\,\mathrm{S\,m^{-1}}$ to $0.1\,\mathrm{S\,m^{-1}}$ as our optimization goal. Low values of ε_r and σ correspond to a low moisture concrete. A maximum antenna area of 4 cm × 10 cm is chosen as the boundary condition and the individual pixels/crosses have a size of 2 mm. The antenna's substrate is ROGERS RO4350B with a thickness of 0.50 mm and it is covered with a 2 cm layer of concrete on top and a 15.5 cm layer of concrete on the bottom.

The resulting antenna is depicted in Fig. 3.

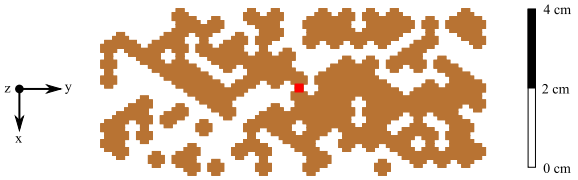

FIGURE 3. Optimized pixelated antenna for operation within concrete. It has a size of 97 mm × 42 mm.

As described above, the optimization flow employs Sonnet software, due to its fast computing time. The concrete layers fill the whole simulation room in width and length which are chosen to be 2.7 × λ, for optimum simulation accuracy. However, the blocks as chosen in the experiments have a size of 30 cm × 30 cm × 17.5 cm. Therefore, in order to verify the optimization results obtained with Sonnet, Ansys HFSS is used to simulate the antenna's characteristics with the same block size as used in the experiments, due to its accuracy. Consequently, all simulation results shown in this work have been obtained with Ansys HFSS.

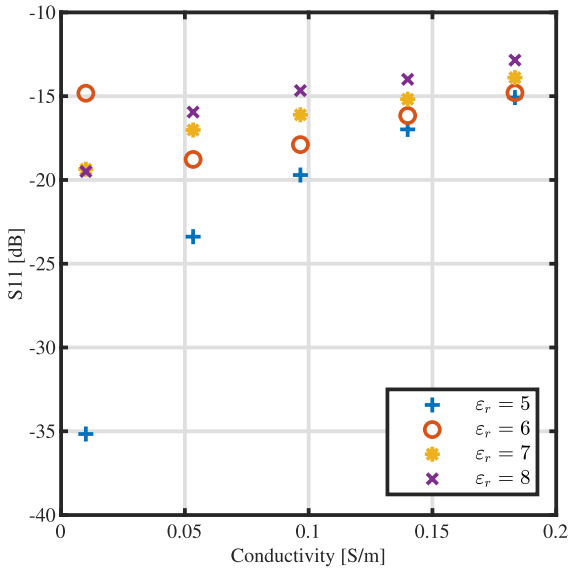

FIGURE 4. Simulated S11 parameters at 868 MHz for various concrete material parameters. S11 is evaluated for a variety of values of permittivity and conductivity, which are expected for concrete in various conditions from literature.

A. SIMULATION RESULTS

Fig. 4 depicts the simulated S11 parameter at 868 MHz for different values of ε_r with respect to σ. It can be seen that

TABLE 2. Fresh concrete properties.

Property	Test Setup	Measurement	Criteria	Category
Consistency	Flow Table Test	350 mm to 410 mm	410 mm	F38
Water Content	Microwave Oven	w/cm = 0.44	w/cm = 0.45	XC4/XD3/XF4
Air Content	Pressure Method	6.0 %Vol. to 10.0 %Vol.	6.8 %Vol.	XF4
Bulk Density	-	-	2277 kg m^{-3}	

the antenna is operational over the whole range of expected concrete properties.

For all permittivities, a reflection coefficient of at least −12 dB is observed. Additionally, as expected the S11 parameter increases with increasing conductivity and permittivity.

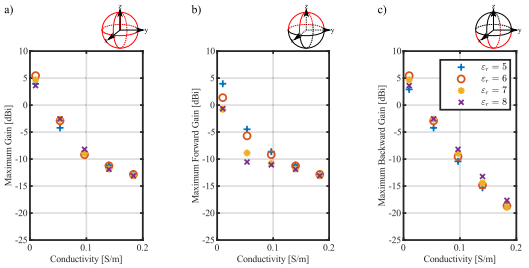

FIGURE 5. Maximum antenna gain evaluated for all angles θ and ϕ in A), for only positive z values $\theta \in [0, 90]$ in B) and for negative z values $\theta \in [90, 180]$ in C).

Furthermore, the gain was simulated for different values of ε_r with respect to σ in the two elevation and the azimuth cuts. The results for the maximum antenna gain are shown in Fig. 5. Additionally, a separation in forward and backward direction is performed.

The maximum antenna gains occurring at elevation ($\varphi = 0, 90\,^\circ$ and $\vartheta \in [0, 180]\,^\circ$) and azimuth angles ($\varphi \in [0, 360]\,^\circ$ and $\vartheta = 90\,^\circ$) are shown in Fig. 5-a). Increasing conductivity values lead to higher electrical losses within the concrete. Therefore it can be seen, that the gain decreases rapidly with conductivity, whereas the influence of the permittivity is comparatively low.

The maximum forward gain for elevation with positive z values ($\varphi = 0, 90\,^\circ$ and $\vartheta \in [0, 90]\,^\circ$) is depicted in Fig. 5-b) and the maximum backward gain for elevation with negative z values ($\varphi = 0, 90\,^\circ$ and $\vartheta \in [90, 180]\,^\circ$) is shown in 5-c). It can be seen, that for conductivities below 0.1 S m^{-1} the backward gain is higher than the forward gain. Specifically, for moisture content corresponding to 0.01 S m^{-1} absorption of waves inside the block decreases and reflections at the boundary between concrete and air lead to interference affecting the antenna's properties.

Therefore, the intuitive expectation of increasing antenna gain with decreasing concrete covering, holds only true for high moisture scenarios. For dryer conditions, the correct placement of the antenna within the concrete structure is crucial due to interference from reflected waves inside the concrete. At the expected maximum conductivity of 0.1 S m^{-1}, a gain of minimum −11.1 dBi at $\varepsilon_r = 8$ and −8.6 dBi at $\varepsilon_r = 5$ is observed. For drier conditions, antenna gains as high as −0.65 dBi at $\varepsilon_r = 8$ and 4 dBi at $\varepsilon_r = 5$ are observed.

B. MEASURED RESULTS IN CONCRETE

Measurements have been performed regularly in order to observe the antennas characteristics with respect to moisture and curing time. Fig. 6-a shows the measured moisture values including error bars as a function of the past days since the start of concreting. According to Crank [31] and Künzel [32], diffusion and capillary transport are processes with similar behaviour. They show a linear dependency proportional to the square root of time. Generally, this is valid for various porous materials. Due to its complex pore structure and sealing mechanisms, concrete shows a deviation from this law [33], [34]. Nevertheless, it can be used for a rough estimate in the presented study.

Therefore, the data is also plotted with respect to $1/\sqrt{Days}$ in 6-b. By extrapolating a linear fit to $1/\sqrt{Days} = 0$, it is possible to estimate the equilibrium moisture content. During the first period of time, the majority of the hydration process takes place, which significantly changes water content by chemical binding. Therefore, to justify the assumption of conventional moisture transport for the linear fit, data starting from day 14 is used. In Fig. 6 the linear fit with respect to $1/\sqrt{Days}$ is plotted as a dashed line and the considered data points are indicated by ''x''-Markers.

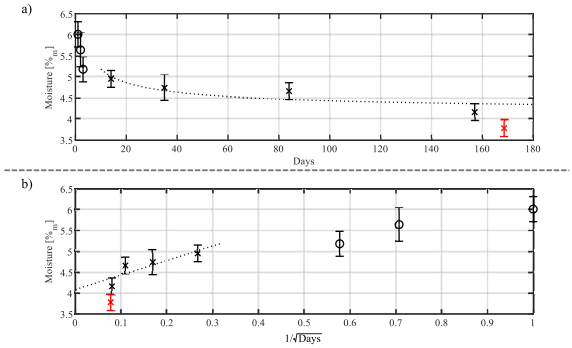

FIGURE 6. Moisture Measurements over time. By extrapolating the $1/\sqrt{Days}$ curve one finds an equilibrium moisture content of 4.084%.

The first measurements have been started 24h after setting the antennas in concrete, as soon as the blocks are hardened sufficiently and the formwork could be removed. Moisture changes the most in the beginning, which is why shorter measurement intervals were used later in the drying process. For each measurement, the moisture is determined as explained

TABLE 3. Comparison of similar published antennas, for operation inside concrete. Values marked with an * are not directly given in cited publications, but calculated and estimated from other given values.

Frequency	Antenna Gain	Volume including airbox cm^3	Volume with respect to wavelength	Moisture	Reference
868 MHz	−1.25 dBi*	3375	$0.082\lambda^3$	not specified	[35]
2.4 GHz	−8.25 dBi	120	$0.062\lambda^3$	day 35 of curing	[15]
2.4 GHz	−6.95 dBi	560	$0.287\lambda^3$	day 35 of curing	[15]
865 MHz	−25 dBi*	32.3	$7.76 \times 10^{-4}\lambda^3$	not specified	[19]
868 MHz	not specified	26.8*	$6.5 \times 10^{-4}\lambda^3$	not specified	[36], [37]
868 MHz	−8.4 dBi	1.63	$3.95 \times 10^{-5}\lambda^3$	4.2 $\%_m$, on day 157	this work

above, in addition to the scattering parameters and antenna gains. In the end the block is gently dried in an oven at 40° to reach a value close to the estimated equilibrium moisture content (red marker).

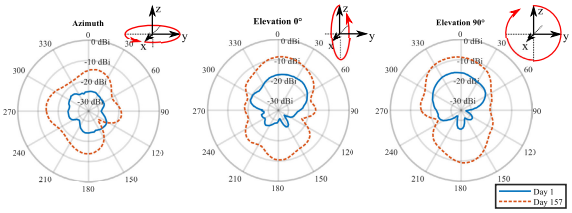

FIGURE 7. Measured gain patterns on day 1 and day 157. The moisture content on the respective days is 6.0% 24h after casting and 4.2% on day 157 in the climate chamber.

Observed Antenna Gain patterns for Azimuth ($\theta = 90°$) and Elevation ($\phi = 0°$ and 90°) are depicted in Fig. 7 for day 1 (Moisture 6.0 %) and day 157 (Moisture 4.2 %). The maximum gain on day 157 is −8.4 dBi, which is significantly higher than on day 1. This behavior is as expected, as a decrease in moisture results in a decrease in conductivity and should therefore lead to an increase of the gain. All measured gains between these days are depicted in Fig. 8, represented by the maximum forward and backward GAIN with respect to measurement day and moisture.

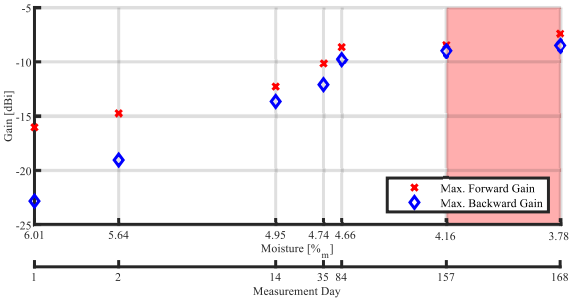

FIGURE 8. Maximum measured forward and backward gain during drying. Similar to fig. 5 a division in forward and backward gain is made. The red box shows a short oven drying period at 40°.

The reflection coefficients are depicted in Fig. 9. At day 1 the S11 parameter has a value of −8.4 dB at the desired frequency of 868 MHz, after 14 days it reaches −10 dB and finally −13 dB is observed after 157 days.

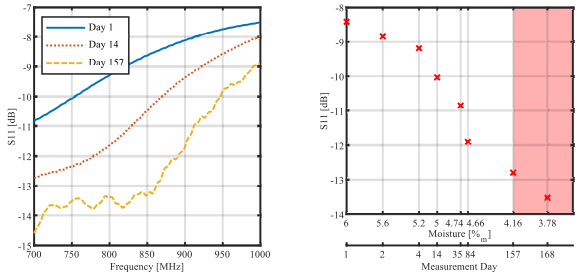

FIGURE 9. Reflection coefficient of the antenna at different stage of drying. On the left broadband measurements are shown on different days of drying, which also reveals the 900 MHz band used in some countries. The right plot shows the S_{11} parameter measured at 868 MHz with respect to the moisture content on those days.

After 157 days of drying in a climate chamber at 22 °C and a relative humidity of 65 %, an antenna gain of −8.4 dBi and a S11 parameter of −13 dB is achieved. These values are expected for typical outdoor conditions in a moderate climate. Measurements after oven drying have shown, that antenna properties will not change significantly for longer drying under the same conditions. It should be noted, that in environments with dryer environmental conditions (or indoors), concrete is expected to dry to much lower moisture content, thus potentially leading to even higher gains.

IV. CONCLUSION AND DISCUSSION

In this study, an antenna for operation in the UHF RFID Frequency bands, completely submerged within concrete, is designed and thoroughly characterized. Due to the fact, that no additional air box is needed for this design, the thickness is given by the employed circuit board substrate. In contrast to approaches that suggest construction of cavities or larger boxes, this allows a much smaller design and a simpler application of sensor devices. In principle, an RFID sensor for structural health monitoring can be build with minimum space requirements, as the electronic components are typically much smaller than the antenna. This minimizes the occupied volume significantly and therefore the impact on the concrete's strength and stability.

In addition to that, the antenna's performance is characterized for a range of moisture contents, that are to be expected for outdoor conditions. As shown previously, concrete parameters such as its moisture content, significantly alter its dielectric properties and as a result also the antenna

performance. Therefore, antennas cured and kept under laboratory conditions may result in very different results in comparison to outdoor structural health monitoring scenarios. However, related works often do not provide information on concrete, curing, environmental conditions or quantify moisture content. In this work the antenna is measured several times during curing, in defined environmental conditions. It has been kept for nearly 6 months in a climate chamber, with values of air humidity close to typical average outdoor conditions. For all measured antenna parameters, also the moisture content has been determined.

A precise quantitative comparison with other work is difficult because the performance depends on a wide variety of parameters and design constraints. Table 3 presents a compilation of other similar studies, where antennas have been designed to be operated embedded inside concrete. Besides the measured antenna gain for in-concrete operation, the volume taken up by the antenna, including any boxes or cavities, is regarded. For the antenna presented by Sidibe et. al. the antenna gain is estimated from measured values for the whole rectenna system [35]. However, the antenna is designed to be operated in a rather large cavity within the concrete with $15 \times 15 \times 15$ cm size, leading to very good results. The second and third entry is the same 2.4 GHz patch antenna with different-sized foam spacer on top [15]. Although, the material losses are expected to be different than at 868 MHz, it can be seen that larger spacers result in higher antenna gain. This work also provides data for the first days after setting in concrete and it can be seen that there is a strong improvement of gain within the first weeks of curing. The two other antennas [19], [36], [37] are part of an RFID sensor tag. Both use a plastic box around the sensor, which creates an air-box. Although a direct comparison of the achieved gain values is not possible, the antenna presented in this work is by far the smallest, as it only consists of the printed circuit board without the need for an additional spacer. This prevents weakening of the mechanical structure by the sensor itself, thus avoiding water ingress.

Considering the moisture content, which is still very high after several months due to the storage at a relative humidity of 65 %, the measured antenna gain is very satisfactory.

Finally, an outlook on potential future usage scenarios of the presented work is given. A possible application is to use the described antenna for UHF RFID based sensing nodes. A rough estimation of possible read ranges can be done using the Friis transmission equation. Using the presented antenna, a theoretical read range of 3.4 m can be achieved, using an exemplary semi-passive transponder with a sensitivity of −15 dBm [19]. A passive sensor system based on the commercially available Rocky100 tag [38] with a typical sensitivity of −10 dBm could achieve a read range of 1.9 m from within concrete. Furthermore, for pure identification scenarios, like detection of unique prefabricated parts, much higher distances can be expected. The antenna itself could be useful for any other sensor node, operating in the same ISM frequency band (e.g. LoRa, IEEE 802.15.4). Further studies will explore the possibility of reading out submerged RFID based sensing nodes in concrete, using the presented antenna optimization method in all-weather conditions, to verify its applicability for real-life scenarios.

It is also worth noting, that the approach presented in section II-B is not limited to concrete, but may be used for arbitrary materials with varying electrical parameters. With the presented optimization scheme it is possible to design antennas for any purpose, where parameters of the surrounding environment are not known precisely, or may vary over a wide range. There are a large variety of applications, where this could be proven useful, such as medical implants inside human tissue. Future studies will focus on the optimization of antennas for the submersion into other materials than concrete.

REFERENCES

[1] G. Koch, *Cost of Corrosion*. Amsterdam, The Netherlands: Elsevier, 2017.
[2] G. M. Calvi, M. Moratti, G. J. O'Reilly, N. Scattarreggia, R. Monteiro, D. Malomo, P. M. Calvi, and R. Pinho, "Once upon a time in Italy: The tale of the Morandi bridge," *Struct. Eng. Int.*, vol. 29, no. 2, pp. 198–217, Apr. 2019.
[3] C. Nuti, B. Briseghella, A. Chen, D. Lavorato, T. Iori, and I. Vanzi, "Relevant outcomes from the history of polcevera viaduct in genova, from design to nowadays failure," *J. Civil Struct. Health Monitor.*, vol. 10, no. 1, pp. 87–107, Feb. 2020.
[4] M. Torres-Luque, E. Bastidas-Arteaga, F. Schoefs, M. Sánchez-Silva, and J. F. Osma, "Non-destructive methods for measuring chloride ingress into concrete: State-of-the-art and future challenges," *Construct. Building Mater.*, vol. 68, pp. 68–81, Oct. 2014.
[5] M. Moosazadeh and S. Kharkovsky, "Development of the antipodal vivaldi antenna for detection of cracks inside concrete members," *Microw. Opt. Technol. Lett.*, vol. 57, no. 7, pp. 1573–1578, Apr. 2015.
[6] S. Sabrin, S. Kharkovsky, and R. Salama, "Dielectric resonator antenna integrated sensors for characterization of concrete," in *Proc. 11th Int. Conf. Sens. Technol. (ICST)*, Dec. 2017, pp. 1–6.
[7] M. A. Islam and S. Kharkovsky, "Detection and monitoring of gap in concrete-based composite structures using microwave dual waveguide sensor," *IEEE Sensors J.*, vol. 17, no. 4, pp. 986–993, Feb. 2017.
[8] J. Cabezas, T. Sánchez-Rodríguez, J. Gómez-Galán, H. Cifuentes, and R. G. Carvajal, "Compact embedded wireless sensor-based monitoring of concrete curing," *Sensors*, vol. 18, no. 3, p. 876, Mar. 2018.
[9] W. D. Leon-Salas and C. Halmen, "A RFID sensor for corrosion monitoring in concrete," *IEEE Sensors J.*, vol. 16, no. 1, pp. 32–42, Jan. 2016.
[10] S. Jiang and S. V. Georgakopoulos, "Optimum power transmission of wireless sensors embedded in concrete," in *Proc. IEEE Int. Conf. RFID (IEEE RFID)*, Apr. 2010, pp. 237–244.
[11] M. N. Soutsos, J. H. Bungey, S. G. Millard, M. R. Shaw, and A. Patterson, "Dielectric properties of concrete and their influence on radar testing," *NDT E Interface*, vol. 34, pp. 419–425, Sep. 2001.
[12] M. R. Shaw, "The permittivity and conductivity of concretes at ground-penetrating radar frequencies," *Adv. Cement Res.*, vol. 10, no. 4, pp. 187–194, Oct. 1998.
[13] B. Filali, F. Boone, J. Rhazi, and G. Ballivy, "Design and calibration of a large open-ended coaxial probe for the measurement of the dielectric properties of concrete," *IEEE Trans. Microw. Theory Techn.*, vol. 56, no. 10, pp. 2322–2328, Oct. 2008.
[14] K. M. Z. Shams and M. Ali, "Wireless power transmission to a buried sensor in concrete," *IEEE Sensors J.*, vol. 7, no. 12, pp. 1573–1577, Dec. 2007.
[15] M. F. Rad and L. Shafai, "Embedded microstrip patch antenna for structural health monitoring applications," in *Proc. IEEE Antennas Propag. Soc. Int. Symp.*, Jul. 2008, pp. 1–4.
[16] X. Jin and M. Ali, "Reflection and transmission properties of embedded dipoles and PIFAs inside concrete at 915 MHz," in *Proc. IEEE Antennas Propag. Soc. Int. Symp.*, Jun. 2009, pp. 28–31.
[17] S.-H. Jeong and H.-W. Son, "UHF RFID tag antenna for embedded use in a concrete floor," *IEEE Antennas Wireless Propag. Lett.*, vol. 10, pp. 1158–1161, 2011.

[18] R. Salama and S. Kharkovsky, "An embeddable microwave patch antenna module for civil engineering applications," in *Proc. IEEE Int. Instrum. Meas. Technol. Conf. (I2MTC)*, May 2013, pp. 27–30.
[19] J.-M. Laheurte, A. Kabalan, H. Retima, E. Piedallu, F. Michelis, and B. Lebental, "Embedded UHF RFID tag for durability monitoring in concrete," *Wireless Sensor Netw.*, vol. 8, no. 7, pp. 137–144, 2016.
[20] D. Mair, M. Renzler, A. Pfeifhofer, and T. Ußmüller, "Evolutionary optimization of asymmetrical pixelated antennas employing shifted cross shaped elements for UHF RFID," *Electronics*, vol. 9, no. 11, p. 1856, 2020.
[21] G. Kiesel and K. Cook, "Optimization of pixelated antennas," in *Proc. IEEE Int. Symp. Antennas Propag. USNC/URSI Nat. Radio Sci. Meeting*, Jul. 2015, pp. 1328–1329.
[22] K. Deb, "Multi-objective optimization using evolutionary algorithms: An introduction Multi-objective optimization using evolutionary algorithms: An introduction," in *Multi-objective Evolutionary Optimisation for Product Design and Manufacturing*, 2001, pp. 1–24.
[23] X. Qing, C. K. Goh, and N. Chen, "Impedance characterization of RFID tag antennas and application in tag co-design," *IEEE Trans. Microw. Theory Techn.*, vol. 57, no. 5, pp. 1268–1274, May 2009.
[24] A. Thomas Milligan, *Modern Antenna Design*. New York, NY, USA: McGraw-Hill, 1985.
[25] *Concrete Specification, Performance, Production and Conformity*, Austrian Standards Institute, Wien, Vienna, Austria.
[26] *Concrete—Specification, Performance, Production, Use and Conformity—Part 1: Rules for the Implementation of OENORM EN 206 for Normal and Heavy Concrete*, Wien, Vienna, Austria.
[27] P. Stemmermann, U. Schweike, K. Garbev, G. Beuchle, and H. Möller, "Celitement—A sustainable prospect for the cement industry," *Cement Int.*, vol. 8, pp. 52–66, 2010.
[28] J. Stark and B. Wicht, *Dauerhaftigkeit von Beton*, 2nd ed. Berlin, Germany: Springer, 2013.
[29] *Testing Fresh Concrete—Part 1 to 12*, Austrian Standards Institute, Wien, Vienna, Austria.
[30] *Test Methods for Concrete—National Application of Testing Standards for Concrete and its Source Materials*, Austrian Standards Institute, Wien, Vienna, Austria.
[31] J. Crank, *The Mathematics of Diffusion*. Oxford, U.K.: Oxford Univ. Press, 1975.
[32] H. M. Künzel, "Verfahren zur ein-und zweidimensionalen Berechnung des gekoppelten Wärme-und Feuchtetransports in Bauteilen mit einfachen Kennwerten," Ph.D. dissertation, Stuttgart, Universität Stuttgart, Germany, 1994.
[33] C. Hall, W. D. Hoff, S. C. Taylor, M. A. Wilson, B.-G. Yoon, H.-W. Reinhardt, M. Sosoro, P. Meredith, and A. M. Donald, "Water anomaly in capillary liquid absorption by cement-based materials," *J. Mater. Sci. Lett.*, vol. 14, no. 17, pp. 1178–1181, 1993.
[34] P. Rucker-Gramm, "Modellierung des Feuchte-und Salztransports unter Berücksichtigung der Selbstabdichtung in zementgebundenen Baustoffen," Ph.D. dissertation, Universität München, München, Germany, 2008.
[35] A. Sidibe, G. Loubet, A. Takacs, and D. Dragomirescu, "Energy harvesting for battery-free wireless sensors network embedded in a reinforced concrete beam," in *Proc. 50th Eur. Microw. Conf. (EuMC)*, Jan. 2021, pp. 3–6.
[36] S. Johann, C. Strangfeld, M. Müller, B. Mieller, and M. Bartholmai, "RFID sensor systems embedded in concrete—Requirements for long–term operation," *Mater. Today, Proc.*, vol. 4, no. 5, pp. 5827–5832, 2017.
[37] C. Strangfeld, S. Johann, and M. Bartholmai, "Smart RFID sensors embedded in building structures for early damage detection and long-term monitoring," *Sensors*, vol. 19, no. 24, p. 5514, Dec. 2019.
[38] *Rocky100 Datasheet DS-ROCKY100-V04*, Farsense, Yorba Linda, CA, USA, 2017.

DOMINIK MAIR (Member, IEEE) received the master's degree in mechatronics from the University of Innsbruck, in 2017, and the Ph.D. degree in technical sciences, in 2021, with the thesis "Optimization of Wireless Communication Systems for the Internet of Things." His research interests include wireless passive systems, antenna optimization, and integrated circuit design of UHF RFID front-ends.

MORITZ FISCHER was born in Innsbruck, Austria, in 1993. He received the bachelor's degree in physics from the University of Innsbruck, Innsbruck, in 2014, the first master's degree in physics from Leopold Franzens University, the second master's degree from the Institute for Ion and Applied Physics, University of Innsbruck, in 2017, and the Ph.D. degree from the Institute of Microelectronics and Implantable Systems. He was worked with the Research Department of Bartenbach GmbH (five-month internship). He is funded by the Doctoral College, Lienz, East Tyrol. His research interests include improving reliability and lifetime of wireless sensor nodes.

JULIAN KONZILIA received the degree in civil engineering from the University of Innsbruck, in 2018. Since then, he has been a Postgraduate Student with the Institute for Concrete Construction and Bridge Design, University of Innsbruck. His research interests include rehabilitation of civil infrastructure and in particular on the durability of textile-reinforced concrete.

MICHAEL RENZLER received the bachelor's degree in physics from Leopold Franzens University, Innsbruck, in 2010, the master's degree in physics from Innsbruck and Linköping, Sweden, in 2013, and the Ph.D. degree from the Nano-Bio-Physics Group, Institute of Ion Physics and Applied Physics, in September 2016, with his dissertation "Electron Interactions with (Doped) Helium Nanodroplets." In October 2016, he joined the Institute of Mechatronics, where he currently holds a position as a Senior Scientist. His research interests include the optimization of antennas and metamaterials and novel manufacturing methods for electromagnetic structures.

THOMAS USSMUELLER (Senior Member, IEEE) was born in Nuremberg, Germany, in 1981. He received the Dipl.Ing. and Dr.Ing. degrees in electrical engineering from the University of Erlangen–Nuremberg, Erlangen, Germany, in 2006 and 2011, respectively. In 2006, he joined as a Research Assistant at the Institute for Electronics Engineering, Erlangen. From 2007 to 2014, he held a position as a Teaching Fellow and the Head of the Chip Design Group, Institute for Electronics Engineering. Since 2014, he has been working as a University Professor with the University of Innsbruck, where he is leading the Group for Microelectronics and Implantable Systems. His research interests include circuits and systems for radio-frequency identification (RFID), analog-to-digital and digital-to-analog converter design, and analog signal conditioning circuits. He is also interested in radio frequency integrated circuit design for ultrawideband and cellular applications. In these areas he has authored or coauthored one book, two book chapters, and more than 130 technical publications.